COMMISSIONING OF NOVOSIBIRSK MULTI-PASS ENERGY RECOVERY LINAC

N.A. Vinokurov, E.N. Dementyev, B.A. Dovzhenko, N.G. Gavrilov, B.A. Knyazev, E.I. Kolobanov, V.V. Kubarev, G.N. Kulipanov, A.N. Matveenko, L.E. Medvedev, S.V. Miginsky, L.A. Mironenko, V.K. Ovchar, V.M. Popik, T.V. Salikova, M.A. Scheglov, S.S. Serednyakov, O.A. Shevchenko, A.N. Skrinsky, V.G. Tcheskidov, Yu.F. Tokarev, P.D. Vobly, Budker INP, Novosibirsk, Russia

Abstract

Novosibirsk energy recovery linac (ERL) facility is planned to use the same RF system and electron gun to run three different FELs. First FEL, installed on the ERL orbit, which lies in the vertical plane, is in operation since 2003. It provides average power up to 500 W in the wavelength range 110 – 240 micron and since 2004 works for users. Four orbits in the horizontal plane were added this year. It is planned to have two additional FELs at the second (20 MeV) and fourth (40 MeV) tracks of ERL. The operation mode with one of three FELs may be chosen by switching of some magnets. Recently the two-orbit mode of ERL (for the second FEL operation) was commissioned successfully. The beam passed four times through the accelerating RF cavities and was absorbed in the beam dump. Thus, the first in the world two-orbit ERL is in operation now. Some details of design, status of the facility and plans are discussed.

INTRODUCTION

A source of terahertz radiation was commissioned in Novosibirskin 2003 [1]. It is CW FEL based on an accelerator–recuperator, or an energy recovery linac (ERL). It differs from other ERL-based FELs [2, 3] in the low frequency non-superconducting RF cavities and longer wavelength operation range. Full-scale Novosibirsk free electron laser facility is to be based on the four-orbit 40 MeV electron accelerator-recuperator (see Fig. 1). It is to generate radiation in the range from 5 micrometer to 0.24 mm [4, 5].

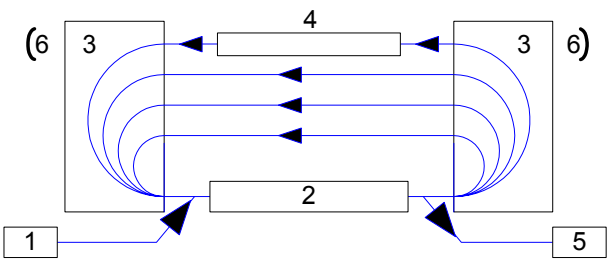

Figure 1: Scheme of the accelerator-recuperator based FEL. 1 - injector, 2 - accelerating RF structure, 3 - 180-degree bends, 4 – undulator, 5 – beam dump, 6 – mirrors of the optical resonator.

THE FIRST STAGE OF NOVOSIBIRSK ERL

The first stage of the Novosibirsk free electron laser (Fig. 2.), based on the energy-recovery linac, generates coherent radiation tunable in the range 110-240 micron as a continuous train of 40-100 ps pulses at the repetition rate of 2.8-22.5 MHz. Maximum average output power is 500 W, the peak power is more than 1 MW [6,7].

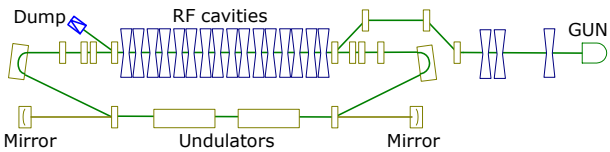

Figure 2: Scheme of the Novosibirsk terahertz free electron laser.

The first stage contains the full-scale 180-MHz RF system and accelerator structure, but has only one orbit. Main parameters of the ERL are summarized in Table 1.

Table 1: Parameters of the first stage of Novosibirsk ERL.

Beam energy, MeV	12
Maximum average electron current, mA	30
RF frequency, MHz	180.4
Bunch repetition rate, MHz	22.5
Bunch length, ps	100
Normalized emittance, mm·mrad	30
Charge per bunch, nC	1.5
RF cavities Q factor	$4 \cdot 10^4$

THE DESIGN OF THE ERL SECOND STAGE

The design and manufacturing of the full-scale four-turn ERL is underway. An artistic view of the machine is shown in Fig. 3. The orbit of the first stage with the terahertz FEL lies in the vertical plane. The new four turns are in the horizontal one. One FEL is installed at the fourth orbit (40 MeV energy), and the second one at the bypass of the second orbit (20 MeV energy).

Some distinguished features of Novosibirsk multi-turn ERL are described below.

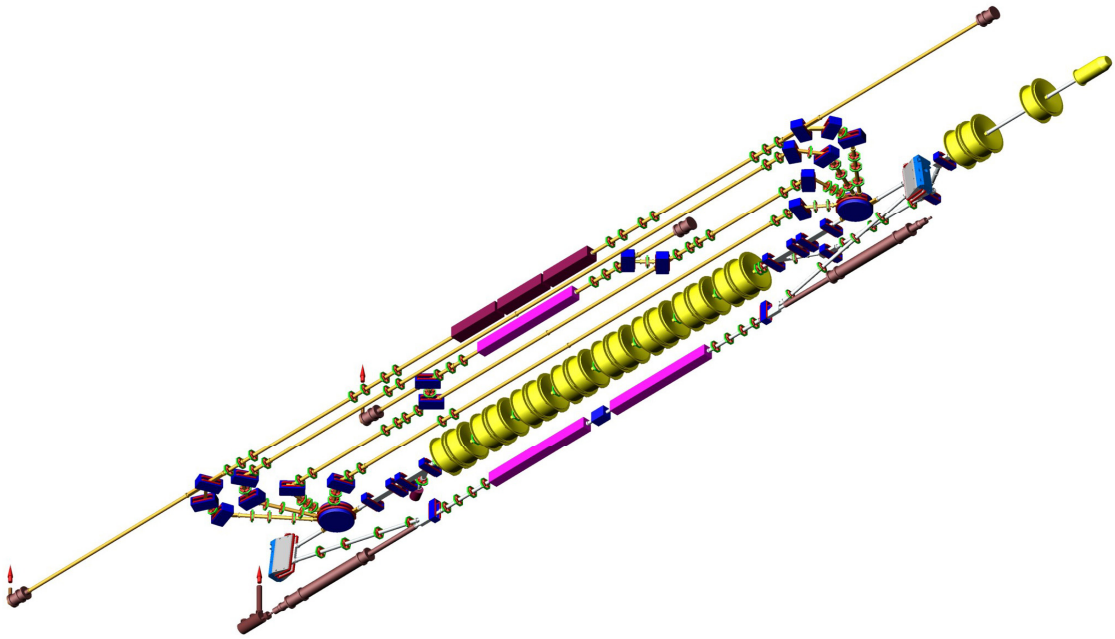

Figure 3: The second stage of the Novosibirsk high power FEL (bottom view).

The Orbit Geometry

It is critical in the realization of the bends that there is one magnet, common for all the passes, which performs separation of the orbits, and there are magnets, different for different orbits, which add the bend to 180 degrees. In the first two paths the rest bending system consists of one magnet. To start with, we'll consider the geometry of the 180° bend, consisting of a round magnet and one bending magnet of the same bend radius. The bend scheme [8] is shown in Fig. 4, where R is bend radius of the magnets, a -radius of the round magnet, d - distance between the axis of the common path and the center of the round magnet, h - height of the path, (π-α) - angle of a bend by the first magnet. Simple geometrical consideration leads to the expression for the bend in the round magnet with homogeneous field

$$\tan\frac{\alpha}{2}=\frac{R-d}{\sqrt{a^2-d^2}}. \qquad (1)$$

It worth noting, that due to axial symmetry round magnet has some advantages. Due to the angular momentum conservation its optical properties are simple. In particular, the second-order aberrations are suppressed. Moreover, as the magnet rotation around the symmetry axis does not matter, the magnet alignment is simple. The separation of trajectories with different energies is rather homogeneous, as the magnetic length increases with energy.

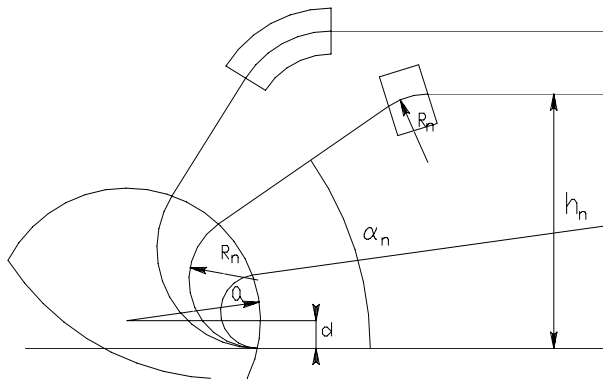

Figure 4: Scheme of the 180° bends with two magnets.

The distance between the round magnet and the second one is $l_0=(h-2R)/\sin\alpha$. Then the total length of the orbit with the bend is

$$S=2L+2\left(\pi R+(h-2R)\tan\frac{\alpha}{2}\right), \qquad (2)$$

where L is the length of the common straight-line section. One can see that the first term $2L$ will be the same for all the orbits, therefore the further consideration will be devoted only to the terms connected with the bends $s = S - 2L$. Substituting expression for $\tan\frac{\alpha}{2}$ (1) to Eq. (2), one has:

$$s=2\pi R+2\frac{(h-2R)(R-d)}{\sqrt{a^2-d^2}}. \qquad (3)$$

Until now we were considering only one orbit. Now we will compare the different orbits. As the particle energy E increases linearly with the number of orbit and the bend

radius in the magnet is proportional to the momentum $p \approx E/c$, the bend radius at the *n*-th pass is

$$R_n = (n+\delta)\Delta R . \quad (4)$$

δ appeared due to the non-zero initial momentum ($\delta = p_0/\Delta p$, where p_0 is the injection momentum, Δp - the momentum gain per pass). For the sake of convenience we shall consider the long straight parts of orbits to be located at an equal distance Δh from each other. Then the height of the *n*-th path is:

$$h_n = h_0 + n\Delta h \quad (5)$$

Substituting expressions for R_n and h_n to Eq. (3), one has:

$$s_n = 2\pi(n+\delta)\Delta R + 2\frac{(h_0 + n\Delta h - 2(n+\delta)\Delta R)((n+\delta)\Delta R - d)}{\sqrt{a^2 - d^2}} . \quad (6)$$

The difference of the lengths of passes *n*+1 and *n*:

$$\Delta s = s_{n+1} - s_n = 2\pi\Delta R + 2\frac{(d-2R_n)(2\Delta R - \Delta h) - \Delta R(2R_{n+1} - h_{n+1})}{\sqrt{a^2 - d^2}} . \quad (7)$$

The particles to come in the same phase at each pass, the difference between passes *n*+1 and *n* should be equal to $q\lambda$ (q is integer, λ is the wave length of accelerating RF).

Then from Eq. (7) we obtain the necessary relation between Δh and ΔR

$$\Delta h = 2\Delta R . \quad (8)$$

Taking into account Eq. (4), (5), (7), and (8), the condition $\Delta s = q\lambda$ can be represented in the form

$$\Delta s = \Delta h\left(\pi + \frac{h_0 - \Delta h\delta}{\sqrt{a^2 - d^2}}\right) = q\lambda . \quad (9)$$

Resolving Eq. (9) for $\sqrt{a^2 - d^2}$, we have:

$$\sqrt{a^2 - d^2} = \frac{h_0 - \Delta h\delta}{q\lambda/\Delta h - \pi} . \quad (10)$$

For our ERL the momentum increase per one pass through the accelerating resonators Δpc is 9 MeV and the injection momentum $p_0 c$ is 1.5 MeV, then $\delta = 1/6$. Choosing the Δh and h_0 to have enough room between parallel straight-line sections, and the angle α_1 for the first orbit, one can find R_n, a, α_n and l_{0n}. Thus, we calculated the whole geometry of the 180-degree bends. To meet the limitation by the accelerator hall width (6 m) and to have reasonable round magnet size *a*, we had chosen *q* = 2.

To provide deceleration after the fourth orbit the length of the last one is different (about 0.7 m longer).

At the second straight line section (abut 20 MeV energy) the bypass with the far infrared FEL is installed (see Fig. 3). The bypass also provides about 0.7 m lengthening of the second orbit. Therefore, when the bypass magnets are switched on, the deceleration of beam take place at the third passing through the accelerating system, and after that electrons come to the first orbit and, after the second deceleration, to the beam dump.

The Mechanical Design

The bends are shown in Fig. 5 and 6.

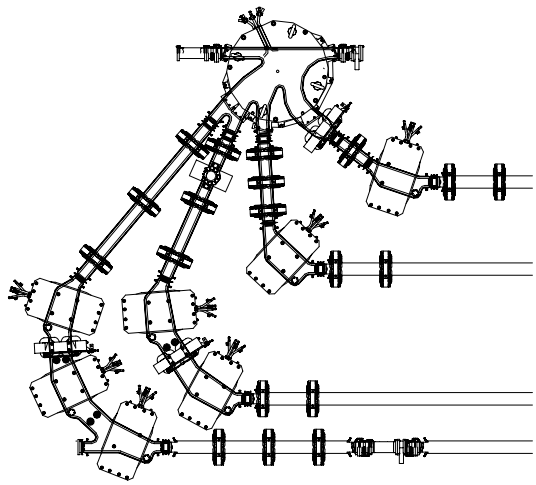

Figure 5: Magnets and vacuum chamber of bends.

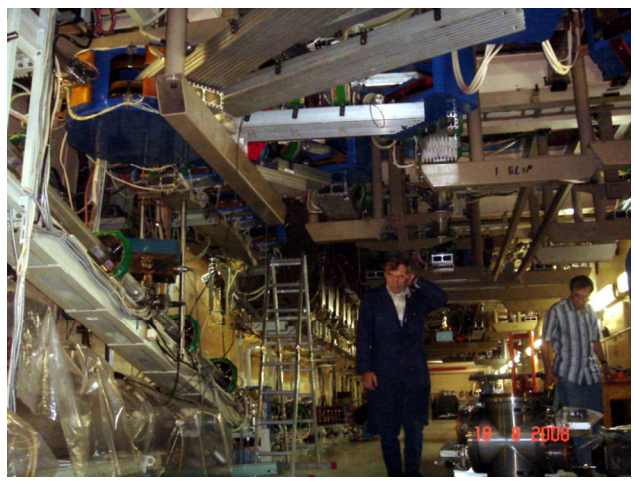

Figure 6: The bends are hanged on the ceiling. Round magnet is at the top left corner, the old teraherts FEL magnetic system is at down-left. Elements of the optical resonator for the second-turn FEL are yet at the floor (down-right corner).

All 180-degree bends are achromatic. To reduce sensitivity to the power supply ripples, all magnets are connected in series. To simplify the mechanical design, all non-round (small) magnets are similar and parallel-edge (see Fig. 7).

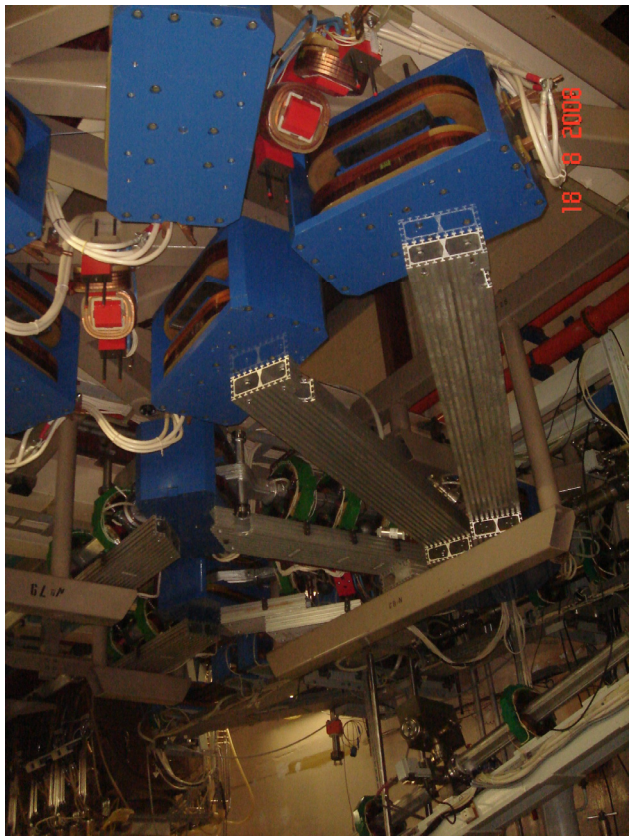

Figure 7: Small bending magnets of third and fourth tracks. Vacuum chambers are not installed yet. Top halves of quadrupoles between bending magnets are seen.

The magnetic field in the small magnets of the first track is about twice lower, than in the round magnets. The magnetic field in other small magnets is twice more, than in the round magnets. It changes slightly the orbit distances from Δh (at fixed orbit lengths), but safe space for focusing quadrupoles and reduce the magnet weight.

Water-cooled vacuum aluminium.

The bypass entrance is shown in Fig. 8. Its magnetic system contains four bending magnets, quadrupoles, and electromagnetic undulator.

CURRENT STATUS

Two first orbits including bypass and undulator were assembled last year. The circulation (two accelerations and two decelerations) of average current 9 mA was achieved. Typical four-turn signal from one of BPM buttons is shown in Fig. 9. This BPM is situated at the accelerating straight section.

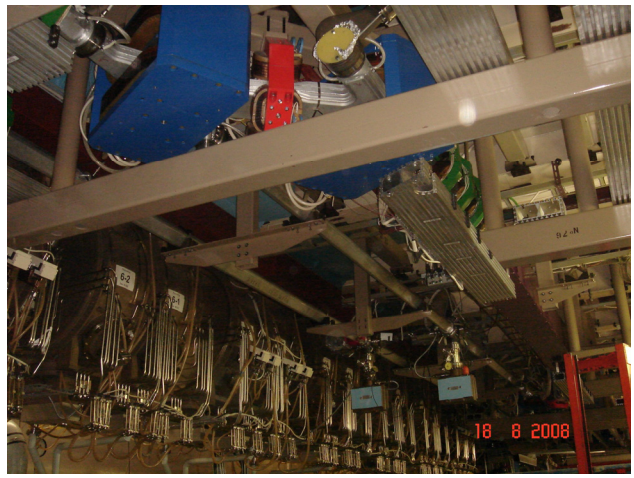

Figure 8: Bending magnets at the entrance of bypass (top). Accelerating RF cavities, vacuum chambers of two first tracks, and undulator (blue) are seen at the lower part of the picture.

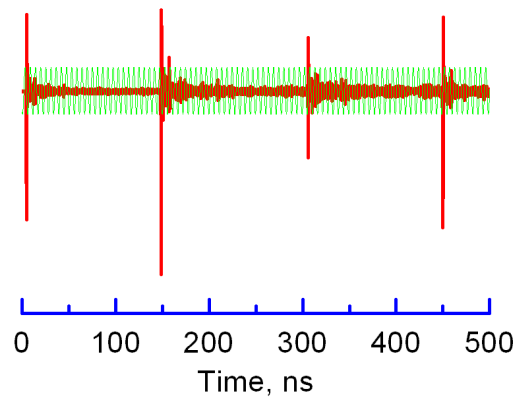

Figure 9: BPM signal of single electron bunch. The sinusoidal RF signal (green) makes possible direct measurement of the orbit lengths.

REFERENCES

[1] E. A. Antokhin et al. NIM A528 (2004) p.15-18.
[2] G.R. Neil et al. Phys. Rev. Lett. 84 (2000), p. 662.
[3] E.J. Minehara. NIM A483, p. 8, 2002.
[4] N.G. Gavrilov et al. IEEE J. Quantum Electron., QE-27, p. 2626, 1991.
[5] V.P.Bolotin et al. Proc. of FEL-2000, Durham, USA, p. II-37 (2000).
[6] V.P. Bolotin et al., Status of the Novosibirsk ERL, NIM A 557, (2006), p.23-27.
[7] E.A.Antokhin et al., Problems of Atomic Science and Technology, p.3-5, №1, 2004.
[8] E.A.Antokhin et al., Proc. of Fourth Asian symposium on free electron lasers (AFEL'99) and Korea – Russia joint seminar on high-power FELs, KAERI, 2000. – P. 221-226.